Targeting JNK3 via Virtual Screening and Molecular Docking to Identify Potential Therapeutic Compounds for Alzheimer's Disease

Zhixin (Jessie) Chen[1]

Received May 22, 2026
Accepted July 21, 2026
Electronic access August 31, 2026

Alzheimer's disease (AD) is a neurodegenerative disease whose current therapeutic approaches remain largely inadequate, as they target single pathways in a complex disease with multiple pathways. Among the most promising targets is c-Jun N-terminal Kinase 3 (JNK3), an enzyme that is the convergence of three key AD pathways: Tau hyperphosphorylation, neuroinflammation, and amyloid-beta accumulation. This study addresses the challenge by applying a computational drug discovery pipeline to identify and evaluate new small-molecule inhibitors of JNK3 with favorable drug-like and safety characteristics. To identify viable JNK3 inhibitors, the study used a computational pipeline for binding site prediction, pharmacophore based virtual screening, molecular docking, drug-likeness evaluation, and toxicity evaluation. Binding site analysis tools were used to identify and confirm the most druggable pocket or regions on JNK3. A virtual screening of commercially available compounds analyzed for molecules matching a pharmacophore model, and the top 15 compounds were further assessed for binding affinity through molecular docking simulations, where the top 6 compounds were advanced to a drug-likeness evaluation using Lipinski's Rule of Five. Based on the toxicity profiling of the top 4 structures from Lipinski's Rule of Five, the pipeline prioritized two lead compounds: Z3361520987 and Z3027289208. These compounds demonstrated strong predicted docking rankings with Gibbs free energy (ΔG) scores of -8.5023 and -8.3053 kcal/mol, respectively, strictly adhered to Lipinski drug-likeness criteria, and displayed acceptable preliminary toxicity profiles. While experimental validation is required as the next step to verify actual functional inhibition and true isoform selectivity, this study begins the foundation for drug discovery and provides a lead for the development of novel molecules for AD.

Keywords: Alzheimer's disease, c-Jun N-terminal Kinase 3, small molecules, molecular docking

Introduction

Alzheimer's disease (AD) is a rapidly expanding public health crisis, currently affecting 7.2 million Americans aged 65 and older. It is currently the seventh leading cause of death in the U.S., and reported deaths from AD increased by 142%.[1] AD causes progressive deterioration of memory and function, often beginning with simple forgetfulness that advances to serious memory loss, difficulty concentrating or thinking, and total loss of functional independence. Currently, there is no cure for AD, but there are treatments to slow the progression of AD or improve symptoms.[2]

Alzheimer's is driven by complex, interconnected pathways. Three such pathways that lead to AD development are the Tau protein pathway, the inflammatory pathway, and the c-Jun N-terminal Kinase (JNK) pathway. In a healthy brain, Tau protein stabilizes the microtubules (i.e., internal skeletal tracks) in neurons, but in AD, Tau becomes excessively phosphorylated, causing it to detach from microtubules. These detached proteins clump together into highly toxic filamentous structures known as paired helical filaments that turn into neurofibrillary tangles, which disrupt the cell's ability to function.[3] Brain studies also show that in AD patients, genes that promote inflammation are elevated, while genes that stop it are inactivated. The level of inflammation is caused by overactivated microglia and buildup of proteins like Amyloid-Beta ($A\beta$).[4] The third key pathway is caused by the enzyme JNK, specifically JNK3, which is the signaling enzyme that responds to cell stress. JNK3 is found primarily in the brain and involved in apoptosis. High levels of $A\beta$ peptides trigger the activation of JNK, which promotes neuroinflammation and the breakdown of brain tissue. Furthermore, it phosphorylates Tau, forming Tau tangles, and studies have shown how blocking JNK in labs has shown to reduce Tau clumping.[5]

Small molecules are essential to AD research and treatments, offering advantages over antibodies due to their ability to cross the blood-brain barrier (BBB). AD is a complex disease with multiple factors and pathways, so single target compounds, such as currently existing ones, are often insufficient and majority focus on decreasing $A\beta$ production and preventing Tau hyperphosphorylation.[7]

[1] *Torrey Pines High School, California, USA*

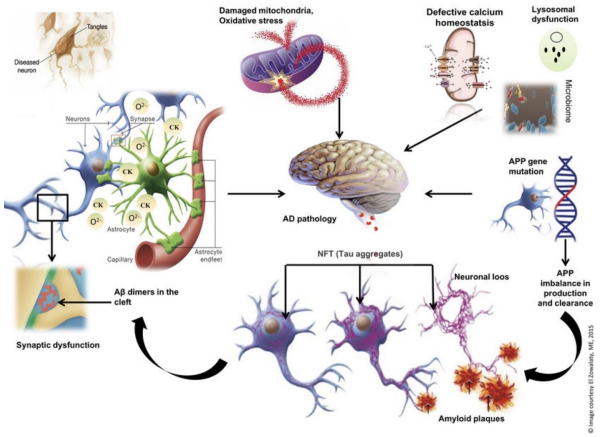

Figure. 1 The image shows the different pathways that can lead to AD, such as Amyloid-Beta plaques (left), Tau tangles (bottom right), mutations and oxidative stress.[6]

JNK belongs to the Mitogen-Activated Protein Kinase (MAPK) family, which regulates essential cell functions. JNK1 and JNK2 are found in almost every tissue of the human body, but JNK3 is found primarily in the brain and central nervous system. Even though treatments target JNK3 for brain diseases, it shares 92% and 87% sequence identity to JNK1 and JNK2, respectively, so its high similarity makes it difficult to develop a drug that only blocks JNK3 without interfering with healthy JNK1 and JNK2 in the rest of the body.[8] Importantly, adenosine triphosphate (ATP) binds within the general kinase cleft situated between the N- and C- terminal lobes, causing ATP-competitive inhibitors frequently facing cross-reactivity challenges across JNK1, JNK2, and JNK3, so isoform selectivity is untested in basic single-receptor screen models.[9] Thus, the compounds designed for AD are designed to compete with ATP, effectively turning the enzyme off. While targeting a junction kinase like JNK3 is conceptually advantageous for multi-pathway modulation, doing so using the ATP-binding pocket introduces cross-reactivity challenges with JNK1 and JNK2, and true isoform selectivity is untested in early-stage models.

JNK3 inhibitors include two types, which are irreversible and reversible depending on how well they bind to the protein. Irreversible JNK3 inhibitors combine with groups in JNK3 using strong covalent bonds, and due to their strength, they cause the enzyme to lose its activity permanently. Reversible inhibitors interact with the enzyme in ways that allow the inhibitor to detach, therefore, the inhibition is not permanent. They bind using non-covalent bonds, such as hydrogen bonds, which are not as stable as covalent bonds, causing the activity level of JNK3 to be lowered rather than lost.[10]

One example of a reversible inhibitor is AS602801 (Bentamapimod), which binds to the ATP-binding site of JNK3, turning the enzyme off. This compound demonstrated that inhibiting the Notch-1/JNK signaling axis highlights a broader protective mechanism against stress-induced neuronal death. Although the study used a trauma and hemorrhage model rather than direct Alzheimer's pathology, it serves as a framework that requires further disease specific validation.[11] However, this treatment is often referred to as a pan-inhibitor, meaning it has the ability to bind to and inhibit JNK1, JNK2, and JNK3. This is risky because JNK1 and JNK2 are found in tissues like the liver, heart, and immune system and are needed for normal cell health.[12]

One example of an irreversible inhibitor is JNK-IN-8, a selective inhibitor that forms a covalent bond with a conserved cysteine residue within the ATP binding site. It was found to be exceptionally potent and inhibited the phosphorylation of c-Jun, a substrate involved in cell death, at sub-micromolar concentration. It targets a specific cysteine residue that the other kinases do not have, so it has higher selectivity than older inhibitors, so it potentially reduces side effects. Furthermore, unlike reversible inhibitors, they provide prolonged effects because they permanently disable the enzyme.[13] However, irreversible inhibitors form permanent covalent bonds, and accidentally binding to the wrong kinase in a non-target tissue could permanently damage the protein's function, posing a major safety concern.[14]

To address these structural and safety challenges, this study aims to computationally evaluate and identify novel small molecule JNK binders as potential therapeutic compounds for Alzheimer's disease. By utilizing a multi-step pipeline of geometric binding pocket prediction, pharmacophore screening, and molecular docking, this work establishes an efficient framework to predict potential novel compounds that could be used for experimental validation.

Methods

Analysis of the druggable binding sites in JNK3

Geometric method for analysis (ProteinPlus)

From the ProteinPlus platform, the module, DoGSiteScorer, was selected for binding site prediction in order to identify and characterize potential binding pockets on JNK3's (Protein Data Bank [PDB] ID: 6EKD) surface.[15]

After choosing the DoGSiteScorer, the option of pockets and druggability were selected for analysis detail and binding site prediction granularity, and all chains were selected. After calculating it, a 3D model of the protein appeared along with a table ranking each pocket by its volume, surface area and drug score (a number from 0 to 1 with higher numbers representing a higher druggability).

Machine learning tool for binding site analysis (PrankWeb)

To combine the shape and energetic requirements for an efficient binding site, the site PrankWeb, a machine learning system for identifying compounds to bind to proteins like JNK3, was used. The same PDB ID was entered with the experimental structure selected for the input method. Then, the system analyzed a model of the protein for its pockets that have high energetic requirements that are ranked.[16]

Analysis of small molecule binders to JNK3

Virtual screening (Pharmit)

To conduct a virtual screening of the JNK3 protein, the software Pharmit was used to generate pharmacophore models based on interactions such as hydrogen bond donors and acceptors, hydrophobic features, and aromatic features.[17] In the website, the same PDB ID was entered, and a pharmacophore model was constructed. When the protein generated, the options hydrophobic, hydrogen donor and hydrogen acceptor were turned on, and in the results, the ligand and receptor were removed. Furthermore, the receptor's surface opacity was turned to zero. Then, Enamine conducted a virtual screening, which across its chemical library contains millions of commercially available compounds. From MolPort, Enamine was used because of the wide availability of compounds and accuracy, where fifteen compounds were selected.

The virtual screening protocol was executed on Pharmit to query large-scale chemical libraries, and the configuration incorporated key pharmacophoric features, specifically hydrogen bond donors and acceptors and hydrophobic centers, derived from the coordinates of the target active site. Pharmit produced a list of compounds ranked by their Root Mean Square of Deviation (RMSD), where a value of 0.000 represents a rigid geometric alignment of a compound's functional group relative to the configured search features. It does not measure or imply binding affinity, structural selectivity, or functional inhibition against the physical JNK3 protein. Screening was conducted using the Enamine database, which uses a default spatial feature tolerance of 0.5 Å to filter the initial library down to the top 15 rigid structural matches.

However, it is important to note that this virtual screening protocol evaluates spatial alignment to the configured pharmacophore features only, and does not evaluate biological selectivity against other JNK isoforms or confirm specific functional inhibition to JNK3.

Analyzing binding affinity of small molecules

Molecular Docking (SwissDock)

SwissDock is a server that performs protein-ligand docking simulations to identify ligand's binding affinity with a specific target protein.[18] The compounds selected from the virtual screening step were utilized for molecular docking analysis, by first using MolPort to find each ligand's SMILES code. The code was entered into SwissDock along with another PDB code for JNK3 (PDB ID: 3FI2) as the target protein. Prior to formal docking simulations, the receptor and ligand structures were standardized using automated server preparation protocols. For the target protein (3FI2), all crystallographic water molecules, co-crystallized ligands, and unrelated heteroatoms were removed to prevent hindrance within the binding pocket. Molecular protonation states and partial charges were assigned a pH of 7.4 using the preparation parameters standard to SwissDock. Compounds were converted from their respective SMILES codes into standardized 3D coordinates. The selected chain was Mitogen-activated protein kinase 10 and no heteroatoms were selected. To cover the entire protein, the box was set to dimensions of 40 x 55 x 29 Å with the center at (21, 29, 5 Å).

The structural transition from PDB ID: 6EKD (from pharmacophore modeling) to PDB ID: 3FI2 (used in molecular docking) was thoroughly evaluated to ensure binding pocket conservation. Both represent high-resolution crystal structures of human JNK3 (6EKD at a 2.2 Å resolution bound to an indazole inhibitor, 3FI2 at 2.4 Å bound to a pyrindinyl-imidazole inhibitor). Structural alignment confirms that the N- and C-terminal lobes remain highly conserved between both conformations, ensuring the search space for the functional ATP-binding site remains consistent despite minor conformation-dependent variations.

While a large-scale matrix evaluation and wet-lab positive control assays were outside the scope of this preliminary computational screen, the specific structural configuration parameters were systematically selected to isolate high-priority binders. Removing all heteroatoms during the automated target preparation step removed native inhibitors and crystallographic solvents from the primary pocket, ensuring unhindered access for new compounds. Furthermore, using an expanded grid search space covering more of the overall structure was intentional to ensure unbiased sampling across the primary terminal without artificial local coordinate constraints. The structural transition between PDB conformations was strictly controlled to preserve the alignment of the core active site.

Because docking simulations were carried out strictly using an isolated JNK3 crystal structure, the results reflect predicted binding metrics within a single-receptor model, and do not account for relative isoform selectivity against JNK1 or JNK2.

Determining drug properties

Analyzing Drug Profiles (SwissADME)

In order to evaluate the drug-likeness of the top compounds after the previous simulation, SwissADME was used to predict pharmacokinetic and drug-likeness properties directly from molecular structure.[19] The SMILES codes for the compounds were retrieved from MolPort and entered individually into the SwissADME input field. The results were generated and recorded for each compound separately. After running, the compound's molecular weight, LogP value (using the consensus Log $P_{o/w}$), number of hydrogen bond donors and acceptors and number of Lipinski violations were recorded.

Determining toxicity

Toxicity Prediction of Small Molecules (ProTox)

After analyzing which compounds matched with Lipinski's rule of five, the top qualified compounds were then analyzed for their toxicity prediction using Protox.[20] The same SMILES codes for the ligands were inputted into the Tox Prediction software, and all toxicity targets were selected for evaluation. Then each compound was analyzed based off of their predicted LD50 and toxicity class.

Results

Analysis of binding sites

Identifying the correct binding site on a target protein is an important step in drug design, as a suitable binding pocket has to be geometrically compatible with a small molecule, such as being large enough to accommodate the ligand, but enclosed enough to protect it from the solvent.[21]

Using a Difference of Gaussians (DoG) approach from DoGSiteScorer, known for its high accuracy of correctly identifying binding pockets, the protein's surface was scanned to detect pockets, as most binding sites are large, and a small molecule (sizes around 300-500 Da) does not fit the whole thing. The actual drug binds into one specific pocket. The site also ranks them by their DrugScore and looks at features like pocket enclosure, volume, surface area and depth, to prioritize regions for high-affinity to small-molecule binding. In the experiment to find a suitable binding site on the JNK3 protein, DoGSiteScorer successfully identified 15 binding pockets, ranking each with a drug score from highest of 1 to lowest of 0.

A binding pocket's volume is critical as pockets within the range of 300 to 1200 cubic Ångströms ($Å^3$) fit an ideal size range for small molecules. Thus, there are only three pockets — P_0 (1184.26 $Å^3$), P_1 (341.12 $Å^3$) and P_2 (337.6 $Å^3$) — that fall into this range, and they have drug scores of 0.81, 0.83 and 0.44 respectively. Because of P_2's low drug score, it does not fit with the requirements. A lower drug score indicates weaker druggability features, such as a poor enclosure or unfavorable chemical surrounding, which makes it less attractible compared to P_0 and P_1.

Table 1 Analysis of the volume, area, and drug score for the binding sites identified in JNK3 using ProteinPlus.

Name	Volume $Å^3$	Surface Area $Å^2$	Drug Score
P_0	1184.26	1509.97	0.81
P_2	337.6	645.03	0.44
P_1	341.12	586.14	0.83
P_3	239.1	573.5	0.56
P_4	177.41	259.52	0.31
P_8	132.22	253.85	0.23
P_9	119.17	308.61	0.21
P_7	138.43	335.35	0.28
P_6	151.87	148.79	0.56
P_5	163.2	471.04	0.42
P_15	101.06	272.24	0.14
P_14	109.31	242.72	0.25
P_13	110.34	329.96	0.21
P_12	110.66	318.98	0.22
P_11	113.28	213.53	0.26
P_10	113.6	180.26	0.3

Among the multiple pockets identified by DoGSiteScorer, pocket P_0 was prioritized as the target site over P_1 based on structural volume and functional alignment. Pocket P_0 corresponds to the standard ATP-binding site within the cleft between the N- and C- terminal lobes, leading to a highly favorable drug score and optimal spatial volume required to accommodate small molecules. Conversely, pocket P_1 represents a smaller, superficial allosteric site, and because competitive inhibition of the ATP pocket is the mechanism for turning off kinase signaling pathways, pocket P_1 was eliminated.

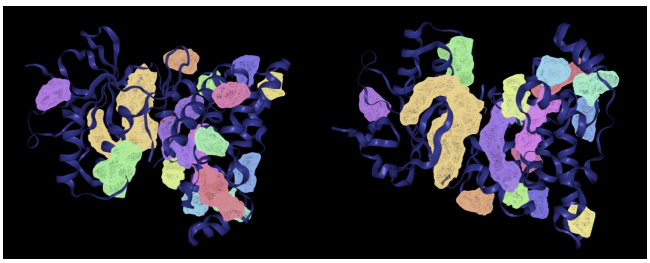

Figure. 2 Different angles of binding sites on JNK3 (PDB ID: 6EKD) rendered using ProteinPlus. The blue ribbon structure represents the JNK3 and the colored spheres represent the binding sites.

Along with having proper geometric requirements, it is also important to consider the energetic factors because they determine the actual affinity of the interaction, ensuring that a

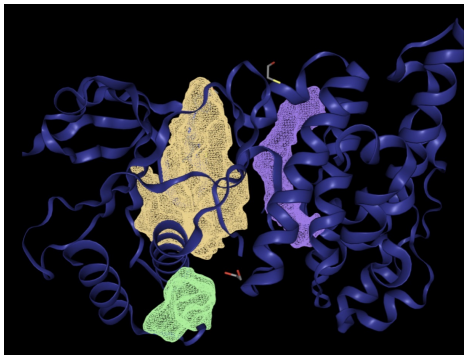

Figure. 3 The binding sites of P_0 (yellow), P_1 (purple) and P_2 (green)

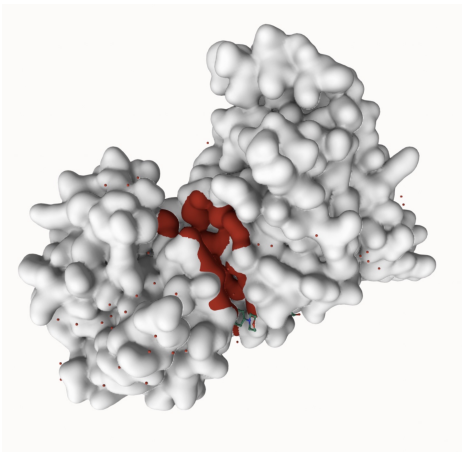

Figure. 4 Image generated by PrankWeb, with red regions indicating high binding potential while white regions represent low predicted binding.

geometrically fitted ligand forms stable and low-energy interactions. They also measure forces like hydrogen bonds, hydrophobic interactions and electrostatics.[22]

Using the P2Rank algorithm, it places thousands of points on the solvent-accessible surface of the protein and scores each point's ability to bind to a ligand based on its surrounding chemical environment. Using PrankWeb, it generated one predicted binding site, with a score of 22.04, probability of 0.859 and 28 residues, representing a strong binding site. The high probability score indicates that the local chemical environment at this site is strongly compatible with protein-ligand binding interfaces observed across thousands of structures. The red coloring in Figure 4 represents residues with the highest predicted binding potential, while the white regions indicate low predicted binding.

The geometric active pocket P_0 identified by DoGSiteScorer structurally overlaps with the 28 residue surface predicted by PrankWeb. The convergence of both independent geometric and energetic approaches from DoGSiteScorer and PrankWeb respectively converging in the same region of the protein validates that both methods are leading to the same ATP-binding site, confirming that this specific pocket is the target environment for docking and drug design.

Binding site identification using DoGSiteScorer and PrankWeb established the foundation for the next steps, and both tools identified the same region (the ATP binding site) of suitable binding sites for JNK3. The site's pockets P_0 and P_1 had high drug scores of 0.81 and 0.83 respectively from DoGSiteScorer combined with PrankWeb's predicted binding probability of 0.859 with 28 residues, validating the site as highly druggable. With the P_0 site from DoGSiteScorer aligning with the site from PrankWeb, the combining of both geometric and energetic approaches increases the confidence that the P_0 pocket is the optimal target for small molecules.

Analysis of small molecule binders

Once the binding sites were analyzed, virtual screening was performed using Pharmit to identify commercially available compounds from the Enamine library that are also geometrically and chemically complementary to the JNK3 binding site.

This was done using a pharmacophore map, which represents a three dimensional model of the molecular features and its spatial arrangement required in order for a ligand to bind effectively, and demonstrates the number of interactions, their distances, and types of interactions.[23]

Figure 5 shows a pharmacophore model for JNK3, which includes a hydrogen bond acceptor in orange and a hydrogen bond donor in white, which reflect the characteristics of the binding pocket. These features are important because hydrogen bond donors and acceptors of the ligand have to align precisely with the protein in order to have a successful interaction.

Fifteen compounds were chosen from the online domain Enamine, and are shown in Table 2. Enamine was chosen because most of the compounds are in alignment with Lipinski's rule of five for evaluating drug properties.

The fit of the compound was determined by the RMSD value, a number from 0 to 1, and is a method to quantify the average distance between the atomic positions of two or more molecular structures. The lower the RMSD is, the greater a similarity between the structures being compared, thus it is a better fit for the binding site. A compound is considered a good fit if the RMSD value is below 0.2, and all 15 compounds have an RMSD value close to zero.

Virtual screening through Pharmit identified 15 compounds from Enamine all with a suitable low RMSD value of 0.000, indicating a perfect alignment with the pharmacophore model of JNK3. This suggested that each compound has the cor-

rect 3D geometry and functional groups (like hydrogen bond donors and acceptors) to interact with the JNK3 binding site, but true isoform selectivity remains untested at this stage. The molecular weights of all compounds also fall within the accepted range for BBB permeability, an important requirement for compounds targeting the brain. All compounds achieved an RMSD of 0.000, confirming that every compound aligns with the pharmacophore model and has the three-dimensional geometry and functional group arrangement to interact with the JNK3 binding site. All compounds also have molecular weights of 231-384 Da, which aligns with the requirement of a weight less than 500 Da, or else the compound might be too large to bind to the protein.

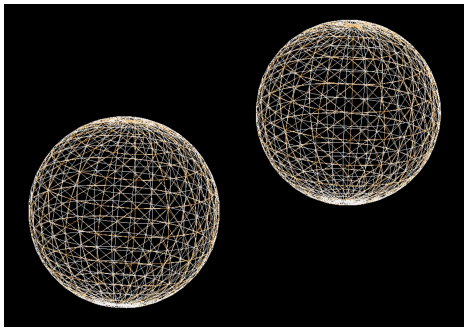

Figure. 5 A pharmacophore map of JNK3 by Pharmit. The orange represents a hydrogen acceptor, and the overlapping white represents the hydrogen donor.

Analysis of Molecular Docking

While pharmacophore screening confirms that the ligand and protein have geometric and chemical compatibility, molecular docking provides a quantitative estimate of how tightly each compound binds to the actual protein structure. SwissDock was used to perform protein-ligand docking simulations using another JNK3 crystal structure (PDB ID: 3FI2). The binding affinities reported across this screening represent the estimated Gibbs free energy (ΔG) of binding, calculated in kcal/mol via the SwissDock scoring function. Within SwissDock, this is referred to as the "SwissParam Score." The more negative the compound was, the more favorable the ligand-protein interaction.[18]

As shown in Table 3, the 15 compounds span a ΔG range of -6.49 to -8.50 kcal/mol, and compounds that meet the threshold of approximately -8.0 kcal/mol or lower were advanced for further evaluation. The ΔG value is consistent with the binding affinities for JNK3 inhibitors, and suggests that the compounds interact with the protein through favorable energetic mechanisms.

However, rather than implementing a rigid threshold of a ΔG score of -8.0 kcal/mol or smaller as a strict exclusionary filter, it was considered as a flexible baseline where compounds clustered around this value were also considered. This explains the inclusion of Z1633030768 (ΔG=-7.9078 kcal/mol), which narrowly misses the benchmark, but its relative performance justifies that it is thermodynamically favorable. From the ΔG score requirements, the six compounds fit this requirement, and were selected for further investigation.

The top-ranked compound, Z3361520987, had the most negative ΔG of -8.5023 kcal/mol, indicating the strongest predicted binding affinity among all potential compounds within this single-receptor model.

Spatial inspection of the top-ranked docking poses confirmed that despite using an expanded grid search space, both lead compounds preferentially settled directly within the primary ATP-binding pocket defined by the N- and C-terminal lobes. The top compound, Z3361520987, successfully docked inside the intended pocket by forming hydrogen-bonding networks and hydrophobic contacts with surrounding residues along the inner walls of the terminal cleft. These target specific interactions confirm that the high-ranking computational scores represent valid, localized binding within the JNK3 active site rather than a non-specific binding to the outer surface of the protein.

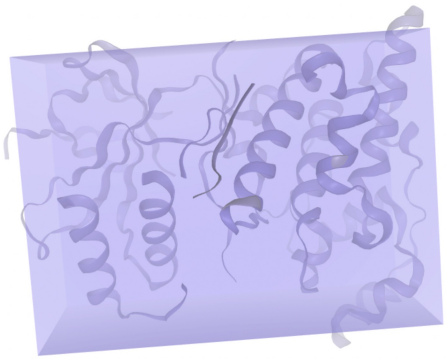

Figure. 6 The docking space of JNK3 with the purple cube as the search space covering most of the protein.

Determining drug properties

To determine whether the top six compounds identified from molecular docking are viable drug compounds, their physicochemical properties were evaluated using SwissADME and analyzed using Lipinski's Rule of Five. The rule states that a compound is considered drug-like if it has molecular weight of less than 500 Da, a LogP value of less than or equal to 5, no more than 5 hydrogen bond donors and no more than 10 hydrogen bond acceptors.[24]

It is important to consider all of these for different reasons, such as larger compounds are bulkier and are unable to pass

Table 2 15 selected drug compounds ranked from lowest to highest RMSD value.

Name	RMSD	Mass	Rotatable Bonds (RBnds)	Overlay of the compound on the pharmacophore map
Z4662064535	0.000	384	6	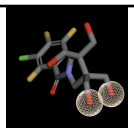
Z1633030768	0.000	301	3	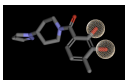
Z1270419575	0.000	283	5	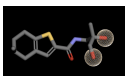
Z3345492012	0.000	302	5	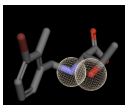
Z1835964693	0.000	374	7	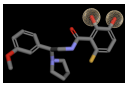
Z56177597	0.000	366	5	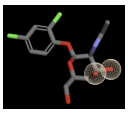
Z2447262340	0.000	305	7	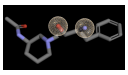
Z2760972589	0.000	315	4	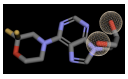
Z3027289208	0.000	346	8	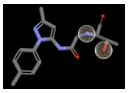
Z1537124450	0.000	231	2	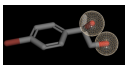
Z1633286604	0.000	343	4	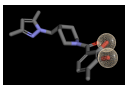
Z3361520987	0.000	317	5	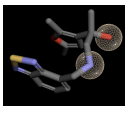
Z2949300531	0.000	318	5	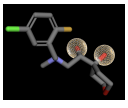
Z2946524941	0.000	286	4	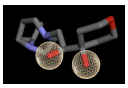
Z4766381161	0.000	333	9	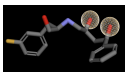

Table 3 Predicted binding affinities of compounds ranked from lowest to highest Gibbs Free Energy values (ΔG), referred to as SwissParam score in SwissDock.

Compound ID	SwissParam Score (ΔG)	Figure
Z3361520987	-8.5023	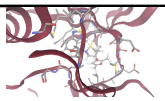
Z1835964693	-8.3993	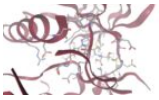
Z3027289208	-8.3053	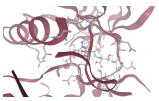
Z4766381161	-8.1964	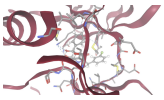
Z1633286604	-8.0531	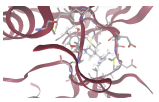
Z1633030768	-7.9078	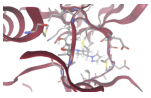
Z2447262340	-7.6711	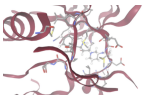
Z3345492012	-7.2931	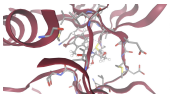
Z2760972589	-7.2737	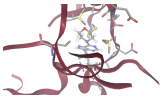
Z4662064535	-7.2387	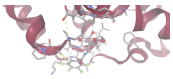
Z56177597	-7.1415	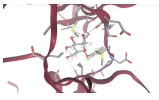
Z1270419575	-6.8237	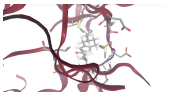
Z2946524941	-6.6212	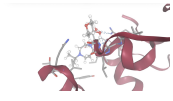
Z1537124450	-6.5657	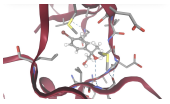
Z2949300531	-6.4901	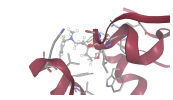

Table 4 Drug-likeness properties of the top six compounds predicted by SwissADME based on Lipinski's Rule of Five.

Compound	Molecular Weight (Da)	LogP	H-Bond Donors	H-Bond Acceptors	Lipinski violations
Z3361520987	317.41	2.59	2	5	0
Z1835964693	374.41	2.72	3	6	0
Z3027289208	346.38	0.13	4	6	0
Z4766381161	333.40	2.49	4	5	0
Z1633286604	343.42	2.55	2	4	0
Z1633030768	301.34	1.61	2	4	0

through cell membranes, so having a smaller compound under 500 Da allows it to cross the BBB to reach the target protein. The LogP measures how lipophilic or hydrophilic a compound is, and a drug needs to have an equal balance to dissolve through fat cell membranes, but also dissolve in the bloodstream, so a value between 0 and 5 accounts for both factors. Hydrogen bond donors and acceptors form strong interactions with water molecules, and having too many of them causes the drug to get trapped with other particles in the body.

As shown in Table 4, all six compounds satisfy all four of Lipinski's criteria without violations, demonstrating excellent drug-likeness profiles for all of them. The compounds' weights fall into the accepted range, ranging from 301.34 to 374.41 Da, which are well below the 500 Da threshold. The LogP values range from 0.13 to 2.72, which are also below the maximum of 5 and above the minimum of 0. Hydrogen bond donor counts range from 2 to 4 and acceptors range from 4-6, both also within Lipinski's limits.

While Lipinski's Rule of Five provides a foundational metric for drug-likeness, compounds targeting Alzheimer's disease require specialized central nervous system (CNS) parameters, like BBB permeability, which remain outside the scope of this preliminary screen.

Analysis of toxicity

Because all the compounds analyzed in the previous experiment meet the four criteria of Lipinski, the top four compounds from molecular docking were selected for further evaluation.

All external compounds that enter the body are toxic to a certain extent, but the goal of this experiment is to evaluate to what extent each compound is toxic to the body. The toxicity of the compound was measured using the predicted LD50 value (standing for lethal dose 50) — representing the estimated amount required to cause death among 50% of the population — and the predicted toxicity class — a number from 1 to 5 with 1 being extremely toxic and a value above 3 being acceptable. The higher the LD50 value, the less toxic the compound is, and a value around 300 is optimal.

All four of the compounds fit in with the LD50 and toxicity class requirements of at least 300 mg/kg for LD50 value and a toxicity class higher than 3. Therefore, the four compounds' toxicity levels meet the baseline requirements, so when choosing which compound is the best fit, the active toxicity areas can be analyzed. Compound Z1835964693 had the most active toxicity areas, specifically nine, and as shown in the chart demonstrating, the respiratory's confidence of positive toxicity exceeds the average of its class (shown by the blue line exceeding the orange region). Compound Z4766381161 had five active toxicity areas, but none of their positive toxicity results exceeded the average for its class. Both compounds Z3361520987 and Z3027289208 have four active regions, with none of them exceeding the predicted average of its class.

However, while the compounds' toxicity levels fall within the standard parameters, these computational values serve strictly as early screening filters. Because they still flagged active risk alerts, these compounds can not be declared "suitable for use" without physiological validation. Furthermore, the toxicity classes and LD50 values generated must be interpreted strictly as early computational estimates rather than definitive proofs of biological safety. Because the predictive profiling flagged specific alerts, like potential neurotoxicity, respiratory, and cytochrome interactions, these compounds can not be classified as "suitable for use" without extensive experimental validation.

Discussion

This study used a multi-step computational pipeline to identify novel small molecule inhibitors of JNK3 as potential therapeutic compounds for Alzheimer's disease. Through geometric and energetic analysis of the binding sites, virtual screening of pharmacophores, molecular docking and toxicity tests, the fifteen identified compounds were narrowed to four and an overall top compound. Taken together, Z3361520987 is the strongest overall compound. It has the most favorable binding affinity (-8.5023 kcal/mol), satisfies all Lipinski criteria, achieved the highest predicted LD50 of 2000 mg/kg, and has a limited active toxicity profile. Z3027289208 is also a worthy compound for further investigation, with a docking score of -8.3053 kcal/mol, meeting Lipinski criteria and a similar toxicity profile.

Current treatments mainly address single pathways. from reducing amyloid-beta or slowing Tau hyperphosphorylation, which reduce amyloid-beta production or slow Tau hyperphosphorylation, which have limited effects on stopping disease progression.[25] Therefore, these findings offer a potential strategy for AD drug discovery, as JNK is positioned at an in-

Table 5 Top four compounds from molecular docking analyzed for their LD50 and toxicity class prediction scores, along with the body regions with active toxicity and a chart comparing confidence of positive toxicity results to the average of its classification. The orange region of the chart demonstrates the average active toxicity for active compounds, and the blue represents the compound's active toxicity.

Compound	LD50 (mg/kg)	Toxicity class	Active Toxicity	Chart
Z3361520987	2000	4	Neurotoxicity, Respiratory toxicity, BBB-barrier, Pregnane X receptor (PXR)	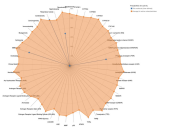
Z1835964693	562	4	Neurotoxicity, Nephrotoxicity, Respiratory toxicity, Immunotoxicity, BBB-barrier, Clinical toxicity, Achetylcholinesterase (AChE), Cytochrome CYP2C9, Cytochrome CYP2D6	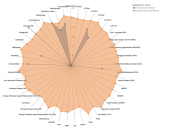
Z3027289208	1300	4	Neurotoxicity, Nephrotoxicity, Respiratory toxicity, Clinical toxicity	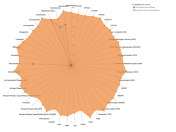
Z4766381161	625	3	Nephrotoxicity, Respiratory toxicity, Cardiotoxicity, BBB-barrier, Clinical toxicity	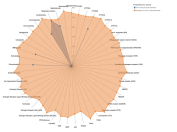

tersection of the three major AD pathways, and a compound inhibiting JNK3 then has the potential to target all pathways, making it a more efficient strategy over existing single target treatments. Moreover, the computational pipeline offers a cost-effective and time efficient strategy that can be replicated for other disease targets.

While this study provides the computational framework for identifying JNK3 inhibitors, several important limitations should be acknowledged when interpreting the results. For future studies, more compounds, such as up to hundreds, can be tested using the same pipeline. The scale of the experiment is also small, with only 15 compounds tested and evaluated. In future studies, a hundred or more compounds from the Enamine library can be tested using the same steps. With millions of commercially available compounds in the database, the probability of identifying potential compounds increases. Furthermore, the selectivity of the identified compounds across c-Jun N-terminal kinase isoforms has not been computationally or experimentally assessed. Due to the high sequence identity and structural conservation across the JNK family (JNK3 having a 93% similarity with JNK1 and 87% with JNK2), compounds targeting the ATP-binding pocket of JNK3 could present inhibitory activity in JNK1 and JNK2. This could disrupt normal cellular processes and JNK1 and JNK2 serve important roles in regulating cellular processes, disrupting tissues in the liver, heart, and immune system that could lead to adverse effects. Consequently, these compounds cannot be classified as definitively selective based on single-receptor docking models. Further analysis can be done with JNK1 and JNK2, specifically sequence-structure alignments against JNK1 and JNK2 to map unique pocket variation and comparative cross-docking, is required to evaluate true isoform selectivity across all three JNK isoforms.

It is critical to contextualize that all findings in this study are entirely derived from *in silico* computational modeling and must be interpreted as predicted rankings rather than defini-

tive therapeutic outcomes. The calculated ΔG values serve as a computational tool to prioritize compounds, but they do not equate to the measured experimental binding affinities or established verified inhibition. Before any true therapeutic potential can be claimed, the potential compounds have to go through experimental validation, including formal assays to determine exact LD50 values, selectivity against JNK1 and JNK2, cell-based cytotoxicity screening, and evaluation in Alzheimer's models.

This study used a drug discovery pipeline to identify novel small-molecule inhibitors of JNK3 as potential therapeutic compounds for Alzheimer's disease. These findings demonstrate the power of large chemical libraries for identifying small molecule JNK3 inhibitors, providing a cost-effective and time-efficient alternative for drug discovery approaches. Given the prevalence of AD and the current lack of treatments, JNK3 remains a compelling target to explore, though extensive experimental profiling is required to verify isoform selectivity and true therapeutic potential.

References

1 . A. disease facts and figures, Alzheimer's & Dementia, Vol. 21, pg. e70235, 2025, https://doi.org/10.1002/alz.70235.

2 M. Clinic, Alzheimer's disease - symptoms and causes. https://www.mayoclinic.org/diseases-conditions/alzheimers-disease/symptoms-causes/syc-20350447, 2026.

3 M. Calabrò, C. Rinaldi, G. Santoro and C. Crisafulli, The biological pathways of Alzheimer disease: a review. AIMS Neuroscience. Vol. 8, pg. 86–132, 2020, https://doi.org/10.3934/Neuroscience.2021005.

4 Y. Zheng, X. Zhang, R. Zhang, Z. Wang, J. Gan, Q. Gao, L. Yang, P. Xu and X. Jiang, Inflammatory signaling pathways in the treatment of Alzheimer's disease with inhibitors, natural products and metabolites (review). International Journal of Molecular Medicine. Vol. 52, pg. 111, 2023, https://doi.org/10.3892/ijmm.2023.5314.

5 M. Solas, S. Vela, C. Smerdou, E. Martisova, I. Martínez-Valbuena, M. R. Luquin and M. J. Ramírez, JNK activation in Alzheimer's disease is driven by amyloid and is associated with tau pathology. ACS Chemical Neuroscience. Vol. 14, pg. 1524–1534, 2023, https://doi.org/10.1021/acschemneuro.3c00093.

6 H. E. Marei, A. Althani, J. Suhonen, M. E. E. Zowalaty, M. A. Albanna, C. Cenciarelli, T. Wang and T. Caceci, Recent perspective about the amyloid cascade hypothesis and stem cell-based therapy in the treatment of Alzheimer's disease. Frontiers in Clinical Drug Research. Vol. 5, pg. 144–174, 2016, https://doi.org/10.2174/9781681082318116050006.

7 W. Yao, H. Yang and J. Yang, Small-molecule drugs development for Alzheimer's disease. Frontiers in Aging Neuroscience. Vol. 14, pg. 1019412, 2022, https://doi.org/10.3389/fnagi.2022.1019412.

8 B. M. Swahn, F. Huerta, E. Kallin, J. Malmström, T. Weigelt, J. Viklund, P. Womack, Y. Xue and L. Ohberg, Design and synthesis of 6-anilinoindazoles as selective inhibitors of c-Jun N-terminal kinase-3. Bioorganic & Medicinal Chemistry Letters. Vol. 15, pg. 5095–5099, 2005, https://doi.org/10.1016/j.bmcl.2005.06.083.

9 X. Xie, Y. Gu, T. Fox, J. T. Coll, M. A. Fleming, W. Markland, P. R. Caron, K. P. Wilson and M. S. Su, Crystal structure of JNK3: a kinase implicated in neuronal apoptosis. Structure. Vol. 6, pg. 983–991, 1998, https://doi.org/10.1016/S0969-2126(98)00100-2.

10 Y. Wu, Y. Zhao, Z. Guan, S. Esmaeili, Z. Xiao and D. Kuriakose, JNK3 inhibitors as promising pharmaceuticals with neuroprotective properties. Cell Adhesion & Migration. Vol. 18, pg. 1–11, 2024, https://doi.org/10.1080/19336918.2024.2316576.

11 M. Chen, J. Sun, C. Lu, X. Chen, H. Ba, Q. Lin, J. Cai and J. Dai, The impact of neuronal Notch-1/JNK pathway on intracerebral hemorrhage-induced neuronal injury of rat model. Oncotarget. Vol. 7, pg. 73903–73911, 2016, https://doi.org/10.18632/oncotarget.12094.

12 Q. Wu, W. Wu, V. Jacevic, T. C. C. Franca, X. Wang and K. Kuca, Selective inhibitors for JNK signalling: a potential targeted therapy in cancer. Journal of Enzyme Inhibition and Medicinal Chemistry. Vol. 35, pg. 574–583, 2020, https://doi.org/10.1080/14756366.2020.1720013.

13 T. Zhang, F. Inesta-Vaquera, M. Niepel, J. Zhang, S. B. Ficarro, T. Machleidt, J. Xie, J. A. Marto, N. Kim, T. Sim, J. D. Laughlin, H. Park, P. V. LoGrasso, M. Patricelli, T. K. Nomanbhoy, P. K. Sorger, D. R. Alessi and N. S. Gray, Discovery of potent and selective covalent inhibitors of JNK. Chemistry & Biology. Vol. 19, pg. 140–154, 2012, https://doi.org/10.1016/j.chembiol.2011.11.010.

14 D. S. Johnson, E. Weerapana and B. F. Cravatt, Strategies for discovering and derisking covalent, irreversible enzyme inhibitors. Future Medicinal Chemistry. Vol. 2, pg. 949–964, 2010, https://doi.org/10.4155/fmc.10.21.

15 A. Volkamer, A. Griewel, T. Grombacher and M. Rarey, Analyzing the topology of active sites: on the prediction of pockets and subpockets. Journal of Chemical Information and Modeling. Vol. 50, pg. 2041–2052, 2010, https://doi.org/10.1021/ci100241y.

16 L. Jendele, R. Krivak, P. Skoda, M. Novotny and D. Hoksza, PrankWeb: a web server for ligand binding site prediction and visualization. Nucleic Acids Research. Vol. 47, pg. W345–W349, 2019, https://doi.org/10.1093/nar/gkz424.

17 J. Sunseri and D. R. Koes, Pharmit: interactive exploration of chemical space. Nucleic Acids Research. Vol. 44, pg. W442–W448, 2016, https://doi.org/10.1093/nar/gkw287.

18 M. Bugnon, U. F. Röhrig, M. Goullieux, M. A. S. Perez, A. Daina, O. Michielin and V. Zoete, SwissDock 2024: major enhancements for small-molecule docking with attracting cavities and AutoDock Vina. Nucleic Acids Research. Vol. 52, pg. W324–W332, 2024, https://doi.org/10.1093/nar/gkae300.

19 A. Daina, O. Michielin and V. Zoete, SwissADME: a free web tool to evaluate pharmacokinetics, drug-likeness and medicinal chemistry friendliness of small molecules. Scientific Reports. Vol. 7, pg. 42717, 2017, https://doi.org/10.1038/srep42717.

20 P. Banerjee, E. Kemmler, M. Dunkel and R. Preissner, ProTox 3.0: a webserver for the prediction of toxicity of chemicals. Nucleic Acids Research. Vol. 52, pg. W513–W520, 2024, https://doi.org/10.1093/nar/gkae303.

21 J. Zhao, Y. Cao and L. Zhang, Exploring the computational methods for protein-ligand binding site prediction. Computational and Structural Biotechnology Journal. Vol. 18, pg. 417–426, 2020, https://doi.org/10.1016/j.csbj.2020.02.008.

22 E. P. Raman and A. D. M. Jr., Spatial analysis and quantification of the thermodynamic driving forces in protein-ligand binding: binding site variability. Journal of the American Chemical Society. Vol. 137, pg. 2608–2621, 2015, https://doi.org/10.1021/ja512054f.

23 J. Mortier, P. Dhakal and A. Volkamer, Truly target-focused pharmacophore modeling: a novel tool for mapping intermolecular surfaces. Molecules. Vol. 23, pg. 1959, 2018, https://doi.org/10.3390/molecules23081959.

24 C. A. Lipinski, F. Lombardo, B. W. Dominy and P. J. Feeney, Experimental and computational approaches to estimate solubility and permeability

in drug discovery and development settings. Advanced Drug Delivery Reviews. Vol. 23, pg. 3–25, 1997, https://doi.org/10.1016/S0169-409X(96)00423-1.

25 R. Yarza, S. Vela, M. Solas and M. J. Ramírez, c-Jun N-terminal kinase (JNK) signaling as a therapeutic target for Alzheimer's disease. Frontiers in Pharmacology. Vol. 6, pg. 321, 2016, https://doi.org/10.3389/fphar.2015.00321.